Published in final edited form as:
Heart Rhythm. 2011 February ; 8(2): 244–253. doi:10.1016/j.hrthm.2010.10.020.

Classifying fractionated electrograms in human atrial fibrillation using monophasic action potentials and activation mapping: Evidence for localized drivers, rate acceleration, and nonlocal signal etiologies

Sanjiv M. Narayan, MD, FHRS[*], **Matthew Wright, MBBS, PhD**[†], **Nicolas Derval, MD**[‡], **Amir Jadidi, MD**[‡], **Andrei Forclaz, MD**[‡], **Isabelle Nault, MD, FRCPC**[‡], **Shinsuke Miyazaki, MD**[‡], **Frédéric Sacher, MD**[‡], **Pierre Bordachar, MD**[‡], **Jacques Clémenty, MD**[‡], **Pierre Jaïs, MD**[‡], **Michel Haïssaguerre, MD**[‡], and **Mélèze Hocini, MD**[‡]

[*] University of California and Veterans Affairs Medical Center, San Diego, California

[†] NIHR Biomedical Research Centre at Guy's and St. Thomas' NHS Foundation Trust, London, United Kingdom

[‡] Hôpital de Haut-Lévèque, Bordeaux, France

Abstract

BACKGROUND—Complex fractionated electrograms (CFAEs) detected during substrate mapping for atrial fibrillation (AF) reflect etiologies that are difficult to separate. Without knowledge of local refractoriness and activation sequence, CFAEs may represent rapid localized activity, disorganized wave collisions, or far-field electrograms.

OBJECTIVE—The purpose of this study was to separate CFAE types in human AF, using monophasic action potentials (MAPs) to map local refractoriness in AF and multipolar catheters to map activation sequence.

METHODS—MAP and adjacent activation sequences at 124 biatrial sites were studied in 18 patients prior to AF ablation (age 57 ± 13 years, left atrial diameter 45 ± 8 mm). AF cycle length, bipolar voltage, and spectral dominant frequency were measured to characterize types of CFAE.

RESULTS—CFAE were observed at 91 sites, most of which showed discrete MAPs and (1) pansystolic local activity (8%); (2) CFAE after AF acceleration, often with MAP alternans (8%); or (3) nonlocal (far-field) signals (67%). A fourth CFAE pattern lacked discrete MAPs (17%), consistent with spatial disorganization. CFAE with discrete MAPs and pansystolic activation (consistent with rapid localized AF sites) had shorter cycle length ($P < .05$) and lower voltage ($P < .05$) and trended to have higher dominant frequency than other CFAE sites. Many CFAEs, particularly at the septa and coronary sinus, represented far-field signals.

CONCLUSION—CFAEs in human AF represent distinct functional types that may be separated using MAPs and activation sequence. In a minority of cases, CFAEs indicate localized rapid AF sites. The majority of CFAEs reflect far-field signals, AF acceleration, or disorganization. These results may help to interpret CFAE during AF substrate mapping.

Keywords

Alternans; Atrial fibrillation; Fractionation; Monophasic action potential; Spectral analysis

Address reprint requests and correspondence: Dr. Sanjiv M. Narayan, Cardiology 111A, VAMC/UCSD Medical Center, 3350 La Jolla Village Drive, San Diego, California 92161. snarayan@ucsd.edu.

Introduction

Great strides have been made in understanding the initiation of atrial fibrillation (AF) from triggering ectopy.[1,2] However, the maintenance of AF is far less clear. Accordingly, there is considerable interest in defining "substrates" for ongoing AF and, in particular, whether complex fractionated atrial electrograms (CFAEs) indicate AF-perpetuating sites.[3] In intraoperative human AF studies that support multiwavelet reentry, complex electrograms lay near wave pivot points and regions of slow conduction.[4] Sites consistent with localized AF "drivers" in optically mapped sheep AF also lie adjacent to fractionated electrograms.[5] However, ablating at CFAE sites has demonstrated mixed success in improving outcomes from AF ablation.[3,6]

A central challenge in AF substrate mapping is that CFAE may indicate mechanisms as diverse as rapid local "drivers," wavefront collision, scar, or far-field events.[7,8] Recent studies used virtual unipolar electrograms to map activation at CFAE sites.[9] However, unipolar electrograms may not separate far-field from local activity. Monophasic action potentials (MAPs),[10–13] on the other hand, define local depolarization and repolarization and can identify signals as far field if they are dissociated from local action potentials or fall too early within repolarization to activate local tissue.

We hypothesized that the causes of CFAE in human AF may be separated into rapid localized AF activity, wave collision, or far-field artifact using MAPs to identify local refractoriness, adjacent multipolar catheters to map activation sequence, and spectral analysis. We set out to test this hypothesis in patients prior to AF ablation.

Methods

Study population

We studied 18 patients with symptomatic paroxysmal or persistent AF resistant to antiarrhythmic medications, who were referred for their first catheter ablation procedure. All patients provided written informed consent. Baseline patient characteristics are listed in Table 1.

Electrophysiologic Study and Mapping Protocol

Antiarrhythmic medications were discontinued ≥5 half-lives (30 days for amiodarone) prior to ablation. After conscious sedation, venous access, and transseptal cannulation, patients in sinus rhythm were paced into AF and then mapped after 2 minutes of AF.

Mapping was performed by carefully positioning a 7F MAP catheter (4-mm tip, Biosense-Webster, Diamond Bar, CA, USA) at 11 predetermined biatrial sites in random sequence, adjacent to a quadripolar catheter (3.5-mm tip), a steerable decapolar catheter (5-mm electrode spacing, Xtrem, ELA Medical, Le Plessis Robinson, France) within the coronary sinus (CS), or a duodecapolar pentarray (Bio-sense-Webster, Diamond Bar, CA) or spiral (St. Jude, Sylmar, CA, USA) catheter. Left atrial sites included roof, appendage, left superior pulmonary vein (PV) antrum, right superior PV antrum, septum, posterior wall, isthmus between mitral annulus and left inferior PV, and CS. Right atrial sites included appendage, septum, and cavotricuspid isthmus. Great care was taken to ensure optimum MAP signal quality. AF was recorded for ≥30 seconds at each site (longer if signals were initially unstable). At the conclusion of research mapping, ablation proceeded as previously described.[14]

Surface ECG and intracardiac electrograms were recorded continuously using a digital electrophysiologic recorder (LabSystem PRO, Bard, Natick, MA, USA). MAPs were filtered from 0.05 to 500 Hz, other electrograms from 30 to 500 Hz, and ECG from 0.05 to 100 Hz.

Determination of CFAE and rate

Bipolar electrograms in AF were analyzed for 8.2 seconds on a 100 mm/s scale. CFAEs were defined by reported criteria[15,16] of (1) magnitude <0.5mV; (2) duration >50 ms with >3 deviations from baseline, and/or (3) continuous electrical activity without an isoelectric line, verified visually. Signal voltage was measured in millivolts, and cycle length (CL) was measured manually for 10 AF cycles.[12]

Spectral analysis of bipolar electrograms

Electrograms were analyzed spectrally for 8.192 seconds analyzed for CFAE. Signals were preprocessed[17] using a Hanning window, rectified, smoothed by low-pass filtering at 20 Hz, then transformed using a 8,192-point Fourier transform to compute the power spectrum.

Dominant frequency (DF) was assigned as the largest peak from 3 to 14 Hz. AF regularity was quantified by organization index (OI), the ratio of areas under the DF and its first three harmonics (each for a 1-Hz window) to total spectral area from 2.5 Hz up to but not including the fifth harmonic.[18,19] OI near 1 indicates a narrow peak ("organized" AF), and lower OI indicates broad spectral DF ("disorganized" AF). Figures 1 and 2 show narrow spectral DF (high OI). Figures 3 through 5 show broad spectral DF (low OI).

Stepwise approach to separate CFAE types

Analysis was performed by two investigators (SMN, MW) and included only sites where the best MAPs showed phase 0 (upstroke) and phases I to III (repolarization), without abrupt changes.

This resulted in 124 sites for stepwise analysis. First, to account for episodic CFAE, we identified the most fractionated 8.2-second epoch that we graded as 0 (fractionated for < 25% of epoch), 1 (<50%), 2 (<75%), or 3 (≥75%). Second, we assessed evidence for *localized drivers*, analyzing activation adjacent to CFAE sites for pansystolic sequential patterns or centrifugal radiation.[20,21] Third, we assessed whether CFAE followed AF *acceleration* by comparing adjacent site atrial fibrillation cycle length (AFCL) preceding then during the CFAE epoch. Fourth, we assessed whether CFAE represented *nonlocal (far-field) signals*, indicated by dissociated signals superimposed on MAPs.[7] Finally, we recorded the presence of MAP alternans (≥5% variations in action potential duration [APD] for ≥6 beats[22]), mean plateau MAP amplitude (mV), and location.

Statistical analysis

Continuous variables are expressed as mean ± SD. Categorical variables are expressed as absolute numbers and percentages. In predetermined analyses, we compared CFAE sites consistent with localized rapid drivers against other CFAE types for AFCL, electrogram amplitudes, and other variables using t-tests. Linear regression was used to study the relationship between CFAE (fractionation grade) at each epoch/site and CL. Categorical variables were compared with the Fisher exact test. P <.05 was considered significant.

Results

Table 1 lists patient demographics. We analyzed 124 sites where MAPs met predefined quality criteria (of 198 sites surveyed), reflecting 7 ± 2 sites per patient (6 ± 3 in paroxysmal AF, 7 ± 2 in persistent AF, P = NS). Of these sites, 91 showed CFAE.

Discrete MAPs are common at CFAE sites in AF

Figure 1A shows intermittent CFAE on bipoles D13–14 and D15–16 (red) of a pentarray ("flower") catheter at the base of the right atrial appendage (see fluoroscopy) in a 62-year-old man with persistent AF. Despite irregular rapid CFAE, MAPs were discrete with CL ≈165 ms (similar to A splines) and some morphologic variation. Figure 1B shows CFAE at pentarray electrodes D13–14 to E17–18 near right PVs, with discrete adjacent MAPs and longer than expected CL ≈172 ms (similar to nearby A1–2) in a 28-year-old man with paroxysmal AF. Figure 1C confirms that MAPs reflect local activation, showing discrete MAPs next to nonfractionated signals at CS78 (red), despite CFAE at nearby CS and opposing endocardial sites (pentarray) in a 57-year-old woman with persistent AF. Spectral analysis of the nonfractionated CS78 signal revealed a narrow DF peak.

Stepwise analysis of MAP and activation sequence revealed four patterns of CFAE activation and recovery that are described in the following and summarized in Tables 2 and 3.

CFAE with discrete rapid MAPs and pansystolic local activation

The first CFAE pattern was consistent with localized, rapid, organized AF sites: discrete rapid MAPs with adjacent activation spanning the AF cycle. This was observed in 7 recordings (7.7% of 91 CFAE sites) in five patients, located at the PV antra (n = 4) and posterior left atrial wall (n = 3; Table 3).

Figure 2 shows CFAE at the inferoposterior left atrium in a 66-year-old woman with persistent AF. Fractionation on SP13–14 and SP15–16 (red) and SP1–2 spiral electrodes showed low amplitude (0.1 mV) and duration 128 ms (>75% of CL). Despite near-continuous fractionation (grade 0.75), adjacent MAPs were distinct (albeit variable) with mean CL = 152 ms. Local activation was sequential on spiral catheter SP 1–2 (on time with SP13–14) to SP11–12, spanning >90% of CL (arrowed). Figure 2C shows one hypothetical explanation: CFAE at a slowly conducting zone within a postulated reentrant circuit. Figure 2D shows DF 6.6 Hz with a narrow spectral peak (OI = 0.78), with surrounding electrodes showing a slower rate (DF 6.1 ± 0.5Hz) with lower organization (OI 0.44 ± 0.21).

Overall, CFAE pattern I showed higher OI (0.63 ± 0.15 vs 0.43 ± 0.10; $P = .01$) but similar DF (6.2 ± 0.2 vs 6.0 ± 0.4, $P = .38$) than the adjacent site average. Compared to all other CFAE types in aggregate, CFAE pattern I had lower MAP amplitude (Table 2; $P = .04$), shorter AFCL ($P = .04$), and nonsignificantly higher spectral DF ($P = 0.11$) and bipolar voltage ($P = .17$; Table 2).

CFAE with discrete MAPs after AF acceleration

The second CFAE type had distinct MAPs and occurred after AFCL shortening. This was seen at 7 (7.7%) of 91 CFAE sites, with AFCL shortening from 179 ± 23 ms to 156 ± 32 ms (13% ± 12%, $P = .02$, paired t-test) at the PV ostia, posterior LA, septa, and right atrial appendage (Table 3).

Figure 3 shows AF electrograms at the right atrial appendage ostium in a 62-year-old man with persistent AF, in whom regularized AF was punctuated by CFAE (Figure 3A; lower horizontal lines). On inspection (Figure 3B), AFCL abruptly shortened prior to CFAE, from CL 200 ms without fractionation in epoch 1, to CL 182 ms (9% shortening) with fractionation in epoch 2, to CL 164 ms (18% shortening) with marked fractionation in epoch 3 (B-E pentarray splines). As CL relengthened, CFAE diminished (Figure 3A). Remarkably, MAPs remained discrete during organized AF *and* CFAE, with MAP alternans (upper bar) observed prior to CFAE. Spectral DF showed a broad peak during CFAE (OI = 0.56).

Nevertheless, AF acceleration was not the predominant mechanism for CFAE. We did not observe an inverse relationship between AFCL and fractionation in all recordings (n = 124, $P > .5$) or those with CFAE (n = 91, $P > .5$). MAP alternans were observed prior to 5 of 7 episodes of AF rate-related CFAE.

CFAE due to far-field electrogram detection

The third CFAE pattern had distinct MAPs with dissociated superimposed signals consistent with far-field electrograms. This was seen at 48 (67%) sites at many locations (Table 3).

Figure 4A shows CFAE on the distal radiofrequency catheter (RF) bipole at the left atrial appendage in a 73-year-old woman with persistent AF. Adjacent MAPs (CL ≈ 200 ms) had refractory periods (APD) of 150 to 170 ms in AF. However, additional dissociated signals (black asterisks) are seen that often fell within refractoriness (AP phase 2) and appear to be far field. These signals explain CFAE on the clinical bipole, in this case aligned with a signal on distal RF (red asterisks; red arrows for first four cycles). Spectral DF was broad (OI = 0.50).

Figure 4B shows intermittent CFAE (red arrows) on spiral electrodes SP9,10 and SP19,20 at the right atrial appendage orifice in a patient with persistent AF. Again, dissociated signals (black asterisks) contribute to CFAE on SP9,10 bipole (red arrows) yet were superimposed on local MAPs and often fell within refractoriness. Spectral DF was broad (OI = 0.47). Figure 4C shows a third example of CFAE type III in which intermittent CFAE again are related to electrograms dissociated from the MAPs (asterisks), which likely reflect an admixture of signals on nearby SP1,2 and SP13,14 (red) electrodes.

This third CFAE pattern was commonly observed at left and right atrial septa, which often were fractionated (grade greater than at other sites in aggregate, $P = .04$). Superimposed far field accounted for 88% of CFAE at the septum. The CS also typically showed this CFAE type (Table 3).

CFAE with disorganized local activation

The fourth CFAE pattern lacked discrete MAPs, excluding sites where MAPs were simply difficult to record by including only sites with intermittently discrete MAPs. This pattern arose at 15 (17%) sites (n = 9 patients). Type IV CFAE epochs inconsistently followed AFCL shortening (in 8/15 epochs), with AFCL change from 186 ± 29 ms (pre-CFAE) to 183 ± 31 ms (during CFAE, $P = .40$, paired t-test).

Figure 5 shows MAP and adjacent electrograms at the left atrial septum in a 41-year-old man with persistent AF. After four distinct cycles, CFAE arose concomitantly with loss of discrete MAPs (solid bars) without CL shortening. CFAE then disappeared for two to three cycles and discrete MAPs reemerged. This cycle repeated. In this example, CFAE also arose in the CS and may explain the simultaneous loss of ECG F-wave organization (leads I and II). Spectral DF was broad (OI = 0.66).

CFAE type IV was assigned only after excluding MAP contact issues and other artifacts. Figure 5 shows excellent catheter contact, as evidenced by electrogram amplitudes of 1.5 mV (MAP) and 0.27 mV (RF catheter) and stable inter-CFAE signals. Nonfractionated periods were as short as 1.6 seconds, making respiratory or movement artifact unlikely. Body movement was unlikely given ECG stability.

CFAE compared to other indices

Table 3 indicates the prevalence of each CFAE type at each location, providing an indirect regional assessment of AF substrates. There was no statistically significant difference between induced and spontaneous AF, and no relationship between fractionation grade and left atrial diameter, AFCL, or MAP amplitude (P = NS for each).

Discussion

This study identifies four types of CFAEs in human AF using multipolar catheters and MAPs to define local activation and repolarization and thus identify local from nonlocal (far-field) signals. In general, we found slower more organized activity at CFAEs than expected from their disorganized appearance. Using a stepwise approach, a minority of CFAEs were consistent with rapid localized AF sites and showed discrete MAPs, short CL (≈150 ms), pansystolic activation, narrow spectral DF, and low-signal amplitude. However, most CFAEs (particularly at the atrial septa and CS) reflected far-field signals, AF acceleration, or less-defined disorganization (all with broad spectral DF peaks). These results provide mechanistic insights into the etiology of CFAE and provide a framework to better interpret CFAEs during substrate mapping of human AF.

CFAE with rapid regular and pansystolic activation

Many studies have interpreted pansystolic sequential activation as evidence for microreentry.[4,5] In our study, sites with this CFAE pattern exhibited high narrow DF peaks, low voltage, and rate or organizational stepdown to surrounding sites (Figure 2 and Tables 2 and 3). These features are consistent with rotors in sheep AF,[5] possible AF sources in canine AF,[23] and patients with possible AF drivers.[21] To prove this mechanism, future studies should target ablation at these CFAE type I sites and assess for AF slowing or termination, as off-line analysis in this study precluded real-time ablation.

Acceleration-dependent CFAE

CFAE after AF acceleration (8% of cases) often retained discrete local MAPs and was preceded by APD alternans (Figure 3).

Although rate-related CFAE has been previously reported,[15,24] its mechanisms are unclear. Rate-dependent CFAE may indicate fibrillatory conduction[25] from sources that activate fast enough for “breakdown to AF.” This may result, in turn, from APD restitution slope >1[26] enabling self-amplifying APD alternans, oscillations, and wavebreak. Discrete MAPs and alternans in CFAE type II supports such organized wavebreak rather than nonspecific spatial disorganization. We have also reported APD restitution slope >1[13] and APD alternans[22] as potential mechanisms for human AF. Alternatively, type II CFAE may represent autonomic “bursting” as shown by shortened AFCL and augmented CFAE in dog atria treated with acetylcholine.[27]

Rate dependence may explain attenuated CFAE after PV isolation[24,28] (which slows AF[1]), although when examined for all patients, CFAE did not reflect rate (no inverse relationship with AFCL).

CFAE due to nonlocal (far-field) electrogram detection

Many CFAEs appeared to reflect superimposed far-field signals on bipolar AF electrograms (Figure 4). Using MAPs to categorically mark local activation and repolarization in AF,[12] these signals were clearly dissociated from local activation and often fell within refractoriness, strongly implicating their nonlocal etiology. Although these signals were unrelated to ventricular activation (Figure 4), detailed mapping would be required to locate

their origin in all cases. Intriguingly, this CFAE type III was prevalent at anatomic junctures such as the interatrial septum and CS (Table 3), consistent with this proposed far-field etiology.

Significance of CFAE without discrete MAPs and "disorganized AF"

CFAE without discrete MAPs were observed in 17% of cases (Figure 5) and are difficult to explain. This fourth CFAE type was not consistently preceded by AF acceleration, APD alternans, or other predefined events.

It is possible that MAP disorganization represents spatial disorganization. Although cellular action potentials are distinct during fibrillation,[29] clinical MAPs integrate areas of ≈0.5 cm^2 so that wavebreak, collision, or other disorganization in this field could disrupt MAPs. This hypothesis may also explain why clinical PV isolation (which increases AF organization) reduces CFAE.[24,28] Notably, we defined this type only if CFAEs were interspersed with good-quality MAPs to exclude poor contact.

Clinical implications

CFAE with discrete MAPs, high spectral DF, and low-signal amplitude are rapid localized AF sites, and studies should determine whether ablation at these sites slows or terminates AF or improves postablation outcome. For AF substrate mapping, MAPs identify local activation and re-polarization in AF and thus can identify CFAE due to far-field signals that may be less attractive ablation sites. Rate-related CFAE may be best revisited after PV isolation and/or other ablation steps.

Study limitations

This stepwise approach prioritizes clinical utility (i.e., started by identifying CFAE types indicative of potential AF drivers). However, we accept that different prioritization goals may exist and that these types may not be mutually exclusive. For instance, "localized rapid AF sites" (type I) may also sometimes follow AF acceleration (type II). Although this is the most thorough study to date of multiple-site MAPs in human atria, the PV ostia are underrepresented due to the great difficulty in obtaining good-quality MAPs from those sites. Our decision not to include sites where MAPs were continuously "disorganized" likely underestimates the prevalence of CFAE type IV. Moreover, because monitoring constant contact force currently is not available for MAPs, we accept that our recordings still may suffer from intermittent contact force. We did not remap each site because the protocol already was lengthy, but future studies should study the reproducibility and evolution of CFAE over time. Finally, because MAP analysis was performed offline, we could not ablate at CFAE sites to prove these proposed mechanisms. Finally, the small population reflects limitations in our supply of MAP catheters.

Conclusion

Fractionated electrograms in human AF can be separated into distinct functional types using MAP and activation mapping. Some CFAE types are consistent with rapid localized AF sites, with high and narrow spectral DF and low voltage. Other CFAE types represent far-field electrograms, follow AF acceleration, or may represent spatial disorganization. These data may provide a framework for better understanding of CFAE during AF substrate mapping.

Acknowledgments

Dr. Narayan received funding from Biosense-Webster, the Doris Duke Charitable Foundation, and the National Institutes of Health (R01 HL 83359), and has received honoraria from Medtronic, St. Jude Medical, and Biotronik Corporations. Dr. Narayan is the inventor of intellectual property owned by the University of California relating to AF diagnosis and therapy. Dr. Wright acknowledges financial support from the Department of Health via the National Institute for Health Research (NIHR) Comprehensive Biomedical Research Centre award to Guy's & St. Thomas' NHS Foundation Trust in partnership with King's College London and King's College Hospital NHS Foundation Trust. Dr. Jaïs received research support from Biosense-Webster. This study was supported by Fondation Leducq.

We are grateful to the nursing and technical staff at Hopital Cardiologique du Haut-Lévêque, whose patience and assistance made this study possible.

ABBREVIATIONS

AF	atrial fibrillation
AFCL	atrial fibrillation cycle length
APD	action potential duration
CFAE	complex fractionated electrogram
CL	cycle length
CS	coronary sinus
DF	dominant frequency
MAP	monophasic action potential
OI	organization index
PV	pulmonary vein

References

1. Haissaguerre M, Sanders P, Hocini M, et al. Catheter ablation of long-lasting persistent atrial fibrillation: critical structures for termination. J Cardiovasc Electrophysiol. 2005; 16:1125–1137. [PubMed: 16302892]
2. Chen S-A, Tai C-T, Yu W-C, et al. Right atrial focal atrial fibrillation: electro-physiologic characteristics and radiofrequency catheter ablation. J Cardiovasc Electrophysiol. 1999; 10:328–335. [PubMed: 10210494]
3. Nademanee K, McKenzie J, Kosar E, et al. A new approach for catheter ablation of atrial fibrillation: mapping of the electrophysiologic substrate. J Am Coll Cardiol. 2004; 43:2044–2053. [PubMed: 15172410]
4. Konings K, Smeets J, Penn O, Wellens H, Allessie M. Configuration of unipolar atrial electrograms during electrically induced atrial fibrillation in humans. Circulation. 1997; 95:1231–1241. [PubMed: 9054854]
5. Kalifa J, Tanaka K, Zaitsev AV, et al. Mechanisms of wave fractionation at boundaries of high-frequency excitation in the posterior left atrium of the isolated sheep heart during atrial fibrillation. Circulation. 2006; 113:626–633. [PubMed: 16461834]
6. Oral H, Chugh A, Yoshida K, et al. A randomized assessment of the incremental role of ablation of complex fractionated atrial electrograms after antral pulmonary vein isolation for long-lasting persistent atrial fibrillation. J Am Coll Cardiol. 2009; 53:782–789. [PubMed: 19245970]
7. Narayan SM, Franz MR. Quantifying fractionation and rate in human atrial fibrillation using monophasic action potentials: implications for substrate mapping. Europace. 2007; 9:vi89–vi95. [PubMed: 17959699]
8. Chang SL, Tai CT, Lin YJ, et al. Biatrial substrate properties in patients with atrial fibrillation. J Cardiovasc Electrophysiol. 2007; 18:1134–1139. [PubMed: 17764448]

9. Lo LW, Higa S, Lin YJ, et al. The novel electrophysiology of complex fractionated atrial electrograms: insight from noncontact unipolar electrograms. J Cardiovasc Electrophysiol. 2010; 21:640–648. [PubMed: 20050959]
10. Hertervig EJ, Yuan S, Carlson J, Kongstad-Rasmussen O, Olsson SB. Evidence for electrical remodelling of the atrial myocardium in patients with atrial fibrillation. A study using the monophasic action potential recording technique. Clin Physiol Funct Imaging. 2002; 22:8–12. [PubMed: 12003106]
11. Kim B-S, Kim Y-H, Hwang G-S, et al. Action potential duration restitution kinetics in human atrial fibrillation. J Am Coll Cardiol. 2002; 39:1329–1336. [PubMed: 11955851]
12. Narayan SM, Krummen DE, Kahn AM, Karasik PL, Franz MR. Evaluating fluctuations in human atrial fibrillatory cycle length using monophasic action potentials. Pacing Clin Electrophysiol. 2006; 29:1209–1218. [PubMed: 17100673]
13. Narayan SM, Kazi D, Krummen DE, Rappel W-J. Repolarization and activation restitution near human pulmonary veins and atrial fibrillation initiation: a mechanism for the initiation of atrial fibrillation by premature beats. J Am Coll Cardiol. 2008; 52:1222–1230. [PubMed: 18926325]
14. Takahashi Y, O'Neill MD, Hocini M, et al. Characterization of electrograms associated with termination of chronic atrial fibrillation by catheter ablation. J Am Coll Cardiol. 2008; 51:1003–1010. [PubMed: 18325439]
15. Rostock T, Rotter M, Sanders P, et al. High-density activation mapping of fractionated electrograms in the atria of patients with paroxysmal atrial fibrillation. Heart Rhythm. 2006; 3:27–34. [PubMed: 16399048]
16. Scherr D, Dalal D, Cheema A, et al. Automated detection and characterization of complex fractionated atrial electrograms in human left atrium during atrial fibrillation. Heart Rhythm. 2007; 4:1013–1020. [PubMed: 17675074]
17. Botteron GW, Smith JM. Quantitative assessment of the spatial organization of atrial fibrillation in the intact human heart. Circulation. 1996; 93:513–518. [PubMed: 8565169]
18. Everett TH IV, Moorman JR, Kok L-C, Akar JG, Haines DE. Assessment of global atrial fibrillation organization to optimize timing of atrial defibrillation. Circulation. 2001; 103:2857–2861. [PubMed: 11401945]
19. Hoppe BL, Kahn AM, Feld GK, Hassankhani A, Narayan SM. Separating atrial flutter from atrial fibrillation with apparent ECG organization using dominant and narrow F-wave spectra. J Am Coll Cardiol. 2005; 46:2079–2087. [PubMed: 16325046]
20. Sanders P, Hocini M, JaIs P, et al. Characterization of focal atrial tachycardia using high-density mapping. J Am Coll Cardiol. 2005; 46:2088–2099. [PubMed: 16325047]
21. Krummen DE, Peng KA, Bullinga JR, Narayan SM. Centrifugal gradients of rate and organization in human atrial fibrillation. Pacing Clin Electrophysiol. 2009; 32:1366–1378. [PubMed: 19744279]
22. Narayan SM, Bode F, Karasik PL, Franz MR. Alternans of atrial action potentials as a precursor of atrial fibrillation. Circulation. 2002; 106:1968–1973. [PubMed: 12370221]
23. Ryu K, Shroff SC, Sahadevan J, et al. Mapping of atrial activation during sustained atrial fibrillation in dogs with rapid ventricular pacing induced heart failure: evidence for a role of driver regions. J Cardiovasc Electrophysiol. 2005; 16:1348–1358. [PubMed: 16403068]
24. Lin YJ, Tai CT, Kao T, et al. Spatiotemporal organization of the left atrial substrate after circumferential pulmonary vein isolation of atrial fibrillation. Circ Arrhythm Electrophysiol. 2009; 2:233–241. [PubMed: 19808473]
25. Vaquero M, Calvo D, Jalife J. Cardiac fibrillation: from ion channels to rotors in the human heart. Heart Rhythm. 2008; 5:872–879. [PubMed: 18468960]
26. Weiss JN, Karma A, Shiferaw Y, et al. From pulsus to pulseless: the saga of cardiac alternans (review). Circ Res. 2006; 98:1244–1253. [PubMed: 16728670]
27. Lin J, Scherlag BJ, Zhou J, et al. Autonomic mechanism to explain complex fractionated atrial electrograms (CFAE). J Cardiovasc Electrophysiol. 2007; 18:1197–1205. [PubMed: 17916143]
28. Roux JF, Gojraty S, Bala R, et al. Effect of pulmonary vein isolation on the distribution of complex fractionated electrograms in humans. Heart Rhythm. 2009; 6:156–160. [PubMed: 19187903]

29. Koller ML, Riccio ML, Gilmour RF Jr. Dynamic restitution of action potential duration during electrical alternans and ventricular fibrillation. Am J Physiol. 1998; 275:H1635–H1642. [PubMed: 9815071]

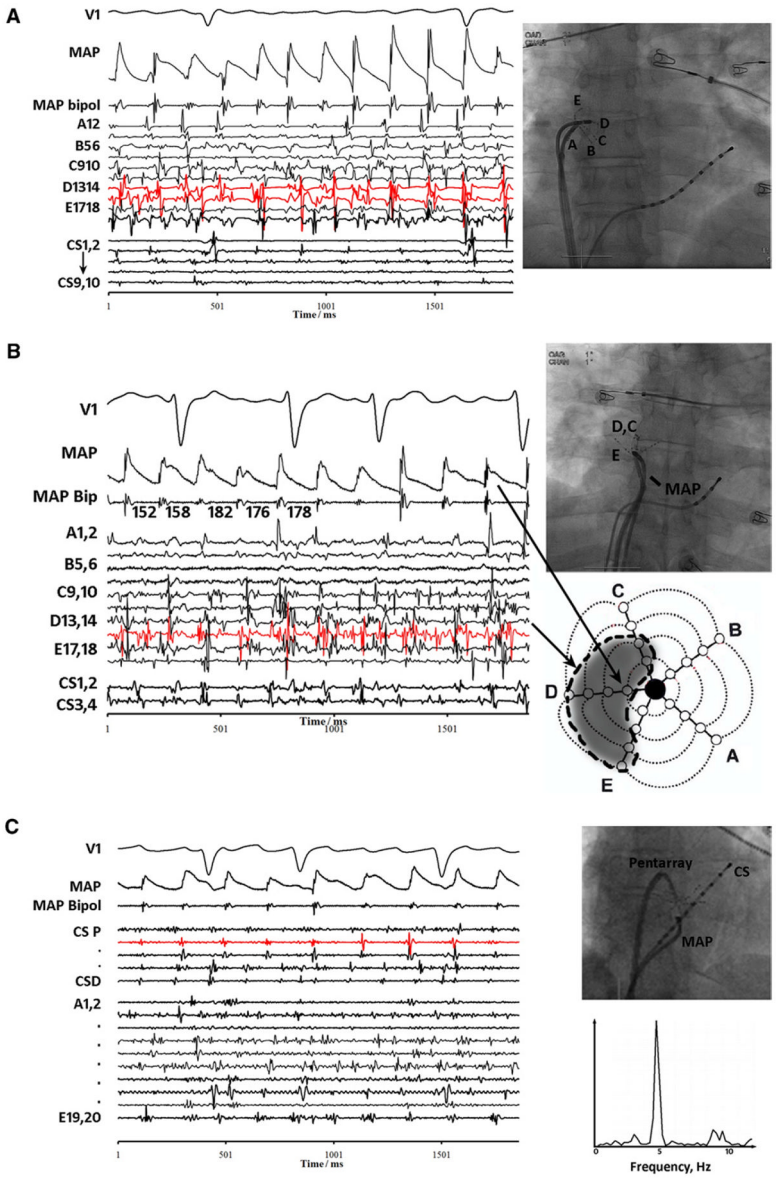

Figure 1.

Discrete monophasic action potentials (MAPs) in human atrial fibrillation, during **(A)** episodic complex fractionated electrogram (CFAE) near right atrial appendage, **(B)** continuous CFAE near right pulmonary vein antra, and **(C)** no fractionation in the coronary sinus (CS78 in *red* and CS56) despite nearby fractionation in the coronary sinus and opposing endocardial surface (pentarray catheter). Spectral analysis of CS78 shows a narrow dominant frequency.

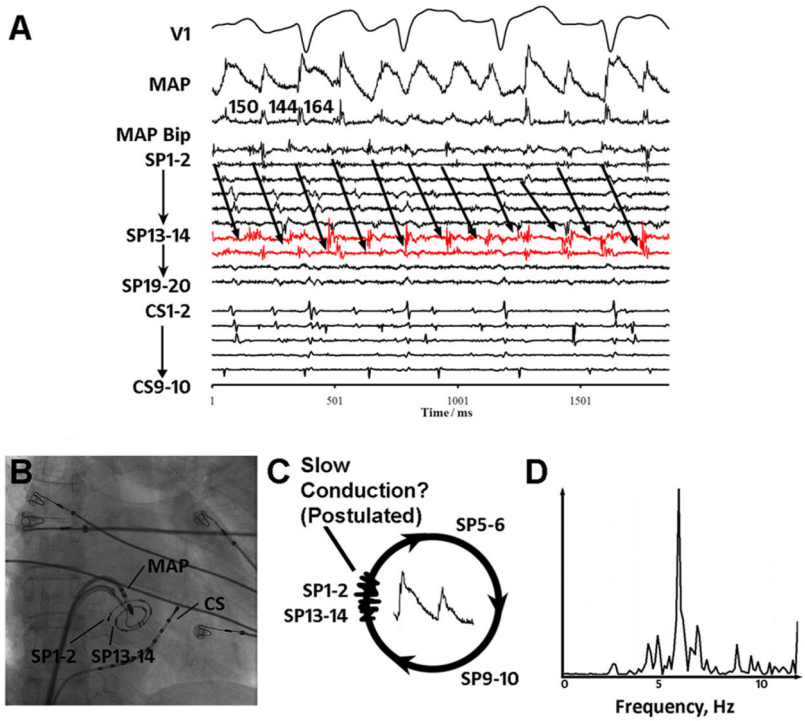

Figure 2.

Complex fractionated electrogram (CFAE) site exhibiting distinct monophasic action potentials (MAPs), rapid rate, and sequential pansystolic activation in atrial fibrillation. **A:** Low posterior left atrium. Low-amplitude CFAEs are seen at SP13–14, SP15–16 *(red)*, and SP1–2 on the spiral catheter. **B:** Fluoroscopy. **C:** Distinct MAPs with sequential activation spanning >90% of the atrial fibrillation cycle length (152 ms), with postulated regions of slow conduction and localized reentry. **D:** Spectral analysis shows narrow dominant frequency at 6.6 Hz.

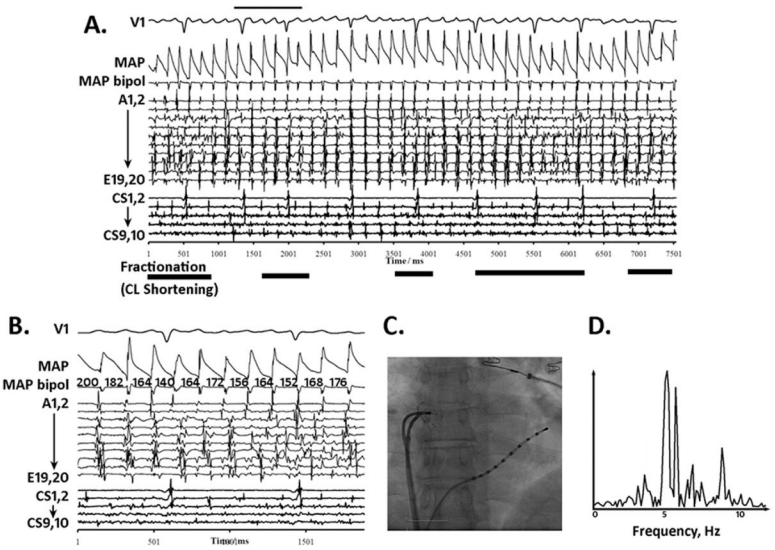

Figure 3.

Complex fractionated electrogram (CFAE) site with distinct monophasic action potentials (MAPs) After atrial fibrillation Acceleration. **A:** Quasi-periodic fractionation in the right atrial appendage *(bold horizontal lines)* punctuate periods of regular activation on pentarray electrograms. MAPs remain distinct throughout. Notably, MAP alternans was observed prior to CFAE *(narrow horizontal bar).* **B:** Abrupt atrial fibrillation cycle length (CL) shortening precedes CFAE. Pentarray splines B–E show CFAE as CL shortens from 200 ms to shorter CL. CFAE attenuated when CL lengthened. **C:** Fluoroscopy. **D:** Spectral dominant frequency is broad.

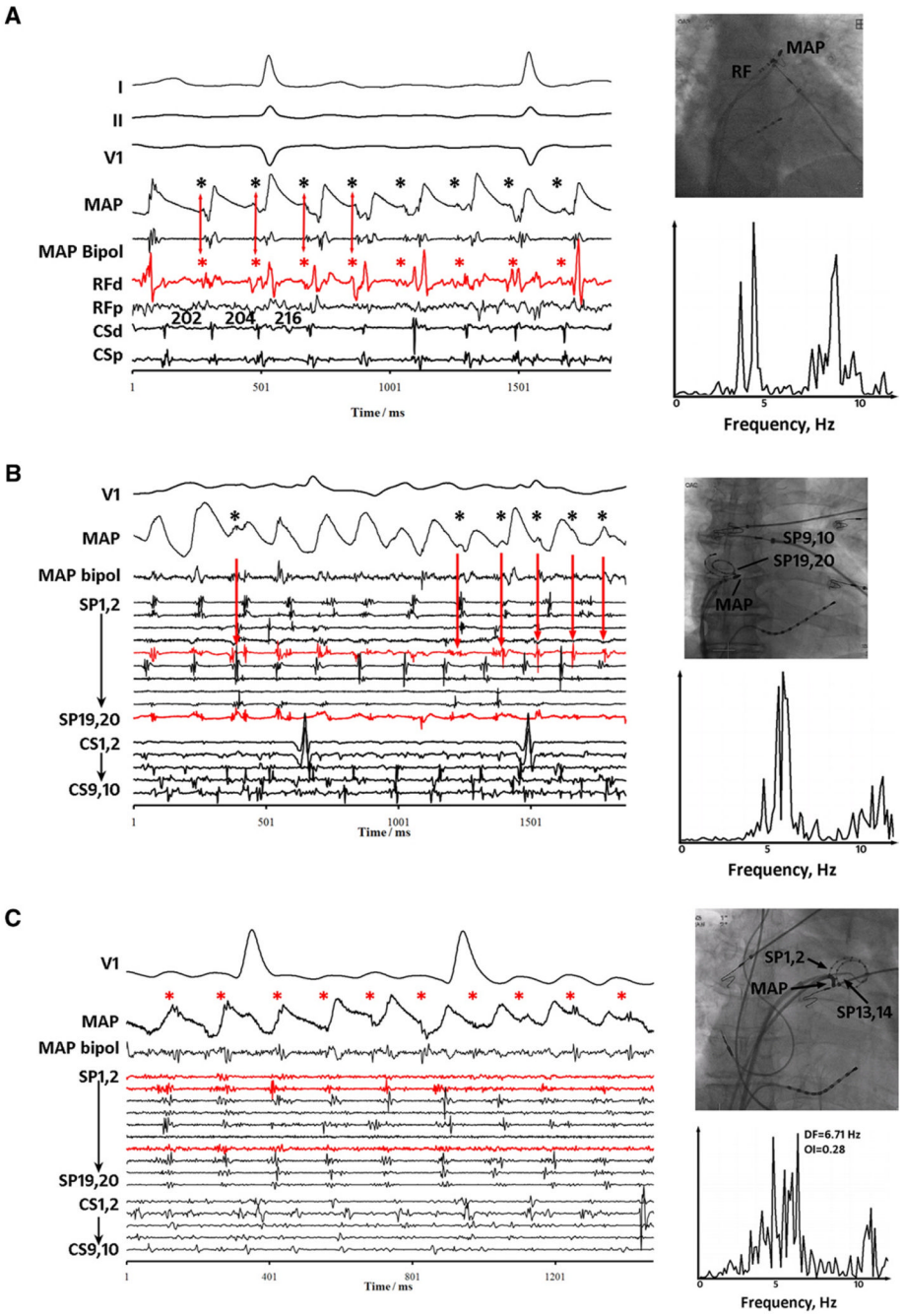

Figure 4.

Complex fractionated electrogram (CFAE) caused by far-field signals (dissociated from local monophasic action potential [MAP]). **A:** CFAE at left atrial appendage base. MAPs adjacent to CFAEs are distinct, reflecting local activation and refractory period (action potential duration 150–170 ms). Superimposed signals *(asterisks)* are dissociated from local activation (MAP), may occur in very early repolarization, and thus appear far field. These signals coincide with RFd (distal RF) signals *(arrows).* **B:** CFAE at the right atrial appendage orifice. MAPs are again distorted by dissociated electrograms *(asterisks)* throughout repolarization that likely are far field, coinciding with signals on SP9,10 and SP19,20 *(red)* of the spiral catheter. **C:** CFAE near left superior pulmonary vein.

Intermittent CFAE timed with small electrograms *(asterisks)* dissociated from local MAP and electrograms on nearby SP1,2 and SP13,14 *(red)* spiral electrodes. In each panel, spectral dominant frequency is broad.

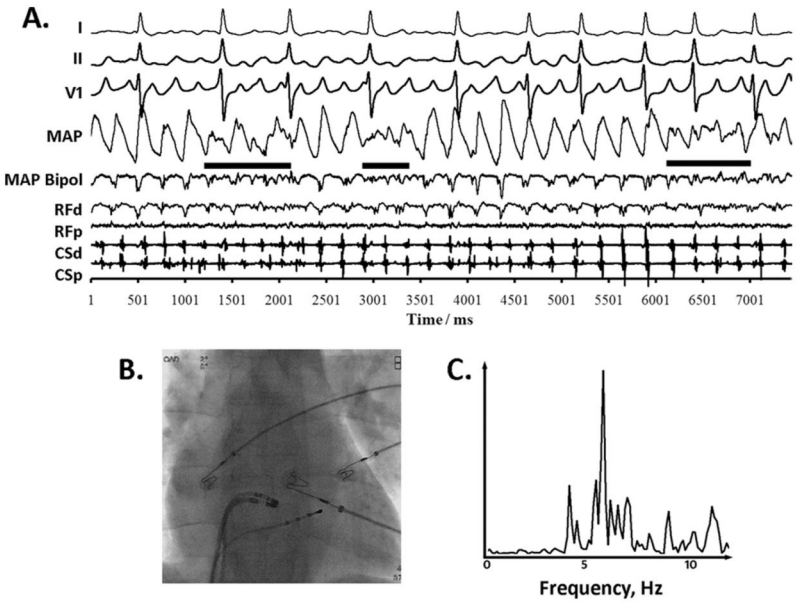

Figure 5.

Complex fractionated electrogram (CFAE) without distinct monophasic action potentials (MAPs) reflecting disorganization. **A:** Quasi-periodic disorganization *(solid horizontal bars)* in bipolar and MAP electrograms at the anterior left atrial septum, alternating with distinct activation in each. MAP alternans precedes the first and second CFAE episodes. **B:** Fluoroscopy. CL Broad spectral dominant frequency peak.

Table 1

Baseline clinical characteristics

Characteristic	
No. patients/no. female	18/7
No. paroxysmal/persistent AF	7/11
Age (years)	57 ± 13
History of AF (months)	91 ± 71
Left atrial diameter (mm)	45 ± 8
LV EF (%)	64 ± 9
LV dysfunction (EF <50%)	1 (6)
Hypertension	8 (44)
Coronary disease (%)	3 (17)
Diabetes mellitus	2 (11)
Prior cardiac surgery	1 (6)
Medications	
RAAS inhibitors	7 (39)
Prior amiodarone therapy	10 (56)

Values are given as mean ± SD or number (percent) unless otherwise indicated.

AF = atrial fibrillation; EF = ejection fraction; LV = left ventricular; RAAS = Renin-Angiotensin-Aldosterone-Axis.

Table 2

CFAE patterns in human AF

Type (%)	Observed regions	Figure no.	AFCL (ms)	Bipolar amplitude (mV)	Bipolar DF (Hz)	Bipolar organization index	MAP amplitude (mV)	MAP DF (Hz)	MAP organization index
I. Rapid activity (8%)	Pulmonary vein ostia, post left atrium	2	157 ± 10*	0.26 ± 0.15	6.2 ± 0.6	0.6 ± 0.1	0.6 ± 0.7*	6.3 ± 0.4†	0.6 ± 0.2
II. Acceleration (8%)	Any site	3	156 ± 32	0.43 ± 0.25	6.6 ± 1.3	0.7 ± 0.2	0.9 ± 0.8	5.9 ± 0.6	0.7 ± 0.2
III. Far-field (67%)	Septum, coronary sinus, all sites	4	185 ± 31	0.40 ± 0.27	5.5 ± 1.1	0.6 ± 0.1	1.0 ± 0.5	5.6 ± 1.0	0.7 ± 0.2
IV. Disorganized (16%)	Any site	5	183 ± 31	0.34 ± 0.24	6.0 ± 1.5	0.6 ± 0.1	0.9 ± 0.8	5.6 ± 1.3	0.5 ± 0.1
V. Not fractionated	Left atrial appendage, right atrial appendage	1C	183 ± 41	0.55 ± 0.51	5.5 ± 1.5	0.7 ± 0.2	1.5 ± 0.9	6.2 ± 2.0	0.7 ± 0.2

AF = atrial fibrillation; AFCL = atrial fibrillation cycle length; CFAE = complex fractionated; DF = dominant frequency; MAP = monophasic action potential.

*P <.05 vs all other CFAE mechanisms.

†P <.10 vs all other CFAE mechanisms.

Table 3

Regional CFAE and electrogram characteristics in human AF

Region	AFCL (ms)	Fractionation grade (0–1)	Prevalence of CFAE types	Bipolar amplitude (mV)	MAP amplitude (mV)
LA appendage	176 ± 38	0.1 ± 0.3	III: 29%, V: 71%	0.6 ± 0.4	1.2 ± 0.7
Pulmonary veins	179 ± 27	0.4 ± 0.4	I: 15%, II: 7%, III: 37%, IV: 19%, V: 22%	0.3 ± 0.3	0.7 ± 0.3
Mitral isthmus	189 ± 35	0.3 ± 0.6	III: 25%, IV: 25%, V: 50%	0.5 ± 0.5	0.9 ± 0.7
LA posterior	187 ± 39	0.5 ± 0.3	I: 15%, II: 5%, III: 60%, IV: 15%, V: 5%	0.3 ± 0.2	0.8 ± 0.4
LA roof	178 ± 35	0.2 ± 0.2	III: 30%, IV: 30%, V: 40%	0.4 ± 0.2	1.2 ± 0.8
Coronary sinus	185 ± 31	0.4 ± 0.3	III: 90%, V: 10%	0.5 ± 0.3	1.0 ± 0.4
LA septum	187 ± 47	0.6 ± 0.2	II: 11%, III: 67%, IV: 11%, V: 11%	0.3 ± 0.2	1.1 ± 0.7
RA septum	180 ± 28	0.5 ± 0.3	II: 22%, III: 56%, IV: 11%, V: 11%	0.5 ± 0.2	1.2 ± 0.5
RA appendage	184 ± 40	0.3 ± 0.4	II: 8%, III: 42%, IV: 8%, V: 42%	0.6 ± 0.6	2.0 ± 0.9
RA high	191 ± 42	0.3 ± 0.3	III: 67%, V: 33%	0.6 ± 0.3	1.5 ± 0.9
RA isthmus	175 ± 29	0.4 ± 0.2	III: 67%, V: 33%	0.4 ± 0.3	1.0 ± 0.5

AF = atrial fibrillation; AFCL = atrial fibrillation cycle length; CFAE = complex fractionated; LA = left atrium; MAP = monophasic action potential; RA = right atrium.